Behavioral/Systems/Cognitive

Small-Conductance Ca^{2+}-Activated K^+ Channel Type 2 (SK2) Modulates Hippocampal Learning, Memory, and Synaptic Plasticity

Rebecca S. Hammond,[1] Chris T. Bond,[3] Timothy Strassmaier,[3] Thu Jennifer Ngo-Anh,[3] John P. Adelman,[3] James Maylie,[2] and Robert W. Stackman[1]

Departments of [1]Behavioral Neuroscience and [2]Obstetrics and Gynecology and [3]Vollum Institute, Oregon Health and Science University, Portland, Oregon 97239-3089

Apamin-sensitive, small-conductance, Ca^{2+}-activated K^+ channels (SK channels) modulate neuronal excitability in CA1 neurons. Blocking all SK channel subtypes with apamin facilitates the induction of hippocampal synaptic plasticity and enhances hippocampal learning. In CA1 dendrites, SK channels are activated by Ca^{2+} through NMDA receptors and restrict glutamate-mediated EPSPs. Studies of SK channel knock-out mice reveal that of the three apamin-sensitive SK channel subunits (SK1–SK3), only SK2 subunits are necessary for the apamin-sensitive currents in CA1 hippocampal neurons. To determine the specific influence of SK2 channels on hippocampal synaptic plasticity, learning, and memory, we used gene targeting through homologous recombination in embryonic stem cells to generate transgenic mice that overexpress SK2 subunits by 10-fold (SK2+/T). In these mice, the apamin-sensitive current in CA1 neurons was increased by approximately fourfold, relative to wild-type (WT) littermates. In addition, the amplitude of synaptically evoked EPSPs recorded from SK2+/T CA1 neurons increased twice as much in response to SK channel blockade relative to EPSPs recorded from WT CA1 neurons. Consistent with this, SK2 overexpression reduced long-term potentiation after high-frequency stimulation compared with WT littermates and severely impaired learning in both hippocampus- and amygdala-dependent tasks. We conclude that SK2 channels regulate hippocampal synaptic plasticity and play a critical role in modulating mechanisms of learning and memory.

Key words: **hippocampus; potassium channel; long-term potentiation; spatial learning; spatial memory; fear conditioning**

Introduction

The hippocampus is an essential brain structure for declarative memory formation that involves memories that can be consciously recollected (Eichenbaum, 2000). In rodent models of declarative memory, lesion studies have demonstrated that the hippocampus is involved in similar memory processes, including learning and remembering complex associations between stimuli (Morris et al., 1982; Squire, 1992; Eichenbaum, 1999). Long-term potentiation (LTP) and long-term depression (LTD) are thought to represent cellular mechanisms of memory formation that involve activity-dependent, long-term changes in synaptic strength and require NMDA receptor (NMDAR) activation (Malenka and Nicoll, 1999).

Small-conductance, Ca^{2+}-activated K^+ channels (SK channels) regulate membrane excitability in CA1 neurons and modulate hippocampal synaptic plasticity and learning (Stackman et al., 2002). SK channels are voltage independent and are activated by submicromolar concentrations of intracellular Ca^{2+} ions. Apamin, a selective SK channel antagonist, enhances the excitability of CA1 neurons (Stocker et al., 1999; Cai et al., 2004). In addition, SK channels regulate synaptically evoked EPSPs. During an EPSP, dendritic SK channels are activated by increases in spine $[Ca^{2+}]_I$, resulting in repolarization of the spine membrane and reinstatement of the Mg^{2+} block of NMDARs (Faber et al., 2005; Ngo-Anh et al., 2005). This SK channel-mediated feedback loop provides one mechanism by which SK channels could regulate hippocampal synaptic plasticity. Consistent with this hypothesis, blockade of SK channels by apamin decreases the threshold for the induction of synaptic plasticity in hippocampal slices (Stackman et al., 2002; Kramár et al., 2004), and systemically administered apamin enhances hippocampal memory encoding (Stackman et al., 2002).

There are three SK channel subtypes (SK1–SK3) expressed in mammalian brain (Kohler et al., 1996). Although all three SK channel subtypes are expressed in the rodent hippocampus, SK1 and SK2 channels are present in layers CA1 and CA3 in significantly higher densities than SK3 channels (Stocker and Pedarzani, 2000; Sailer et al., 2002, 2004). It is unclear from the current literature which specific SK channel subunit(s) contribute to the modulation of hippocampal plasticity and behavior. Transgenic mice, engineered to overexpress or lack one of the three SK channel subtypes, hold great promise for dissecting the unique con-

Received Sept. 27, 2005; revised Dec. 18, 2005; accepted Dec. 21, 2005.

This work was supported by grants from the National Science Foundation (R.W.S.) and National Institutes of Health (J.P.A. and J.M.). We thank Laura Tull, Thanos Tzounopoulos, Paco Herson, Andrey Ryabinin, and Eric Guire for advice and technical support.

Correspondence should be addressed to Dr. Robert W. Stackman at his present address: Department of Psychology, BS 101, Florida Atlantic University, 777 Glades Road, Boca Raton, FL 33431-0991. E-mail: rstackma@fau.edu.

DOI:10.1523/JNEUROSCI.4106-05.2006

 0270-6474/06/261844-10$15.00/0

tributions of each SK channel subtype to specific behavioral and physiological end points. For example, apamin-sensitive currents are absent in CA1 neurons from transgenic mice that lack SK2 subunits (Bond et al., 2004). Therefore, we hypothesize that SK2 channels underlie the apamin-mediated modulation of synaptic plasticity in CA1 neurons and hippocampal-dependent learning. To test this hypothesis, we examined subthreshold EPSPs in CA1 neurons, hippocampal synaptic plasticity, and learning and memory in a transgenic mouse that overexpresses SK2 channels (SK2+/T). The apamin-sensitive current recorded from hippocampal slices in SK2+/T mice was fourfold larger than in wild-type (WT) mice. Consistent with our previous study in which blockade of SK channels enhanced learning, overexpression of SK2 channels impaired hippocampal learning and memory and attenuated subthreshold EPSPs and synaptic plasticity in hippocampal slices. These data support our hypothesis that SK2 channels modulate hippocampal synaptic plasticity and learning.

Materials and Methods

Animals

The Oregon Health and Science University Institutional Animal Care and Use Committee approved all procedures. All mice were group housed and kept on a 12 h light/dark cycle with food and water available *ad libitum*. Mice were weaned at 3 weeks and genotyped. The experimenter was blind to genotype for all behavioral and electrophysiological experiments. Transgenic mouse lines were backcrossed more than six generations onto the C57BL/6J background. For behavioral studies, heterozygous (SK2+/T) mice and WT littermates were used. Male mice were used for all experiments, except the afterhyperpolarization current (IAHP) recordings, and in this experiment, no gender differences were observed.

Transgenic mouse production

A 7 kb *Not*I-*Spe*I fragment positive for hybridization with mSK2 N-terminal coding sequences was isolated from a λ 129/Sv genomic library and cloned into Bluescript as a basis for the targeting construct. Subsequent sequence analysis of overlapping clones revealed the *Not*I site to be vector derived. The tetracycline regulatory cassette (Bond et al., 2000) was inserted 40 nucleotides 5′ of the initiator methionine by homologous recombination in yeast. The resulting targeting construct was electroporated into embryonic stem cells, and G418-resistant colonies were analyzed for appropriate recombination by genomic DNA PCR and Southern blot analysis. Two correctly targeted clones were injected into C57BL/6J blastocysts. One chimera gave germ-line transmission of the tTA allele. SK2 tTA mice were bred to a CRE (cAMP response element) deleter mouse (Bond et al., 2000), resulting in excision of the neomycin coding and yeast URA/3 gene sequences from the allele. The resulting line of mice, mSK2 $tTA_{\Delta neo}$, was maintained as heterozygotes after backcrossing into the C57BL/6J background, with breedings consisting of SK2+/T males crossed with WT females. Although heterozygote SK2+/T mice were viable, produced offspring, and were similar in weight and appearance to WT mice, SK2T/T homozygous mice were not viable without prenatal treatment of doxycycline. For this reason, heterozygous mice were used in each of the present studies.

Western blot

Membrane proteins were prepared from 10- to 16-week-old SK2+/T or WT mice as described previously (Strassmaier et al., 2005). Entire brains were homogenized in ice-cold HS (in mM: 320 sucrose, 10 HEPES, and 1 EGTA) with mammalian protease inhibitor mixture (Sigma, St. Louis, MO). Protein content was determined using the BCA method (Pierce, Rockford, IL). Membrane proteins were mixed in SDS-PAGE loading buffer and separated on an SDS-PAGE gel. Membrane proteins were then transferred onto polyvinylidene difluoride membranes, and anti-SK2-C primary antibody (Bond et al., 2004) was diluted to 2 μg/ml in 3% powdered milk in PBS. HRP-conjugated secondary antibody was diluted 1:10,000 in PBS with 0.1% Tween 20, and blots were visualized with SuperSignal West Pico (Pierce).

Real-time PCR

Whole-brain RNA was isolated with Tri-reagent, and total RNA was reverse transcribed by Moloney murine leukemia virus reverse transcriptase (Invitrogen, Carlsbad, CA), as reported previously (Bond et al., 2004). Expression levels of real-time PCRs were determined by comparison with 18S ribosomal RNA (RNA) and performed in triplicate. The amplicon for 18S was 76 bp (primers: CCGCAGCTAGGAATAATGGA, CCCTCTTAATCATGGCCTCA), for SK1 was 118 bp (primers: GCTCTTTTGCTCTGAAATGCC, CAGTCGTCGGCACCATTGTCC), for SK2 was 151 bp (primers: GTCGCTGTATTCTTTAGCTCTG, ACGCTCATAAGTCATGGC), and for SK3 was 148 bp (primers: GCTCTGATTTTTGGGATGTTTG, CGATGATCAAACCAAGCAGGATGA). The threshold cycle (Ct) indicates the fractional cycle number at which the amount of amplified target reaches a fixed threshold. The reaction master mix, consisting of 1× buffer, Mg (C_f = 4 mM), deoxyribonucleotide triphosphates (C_f = 200 μM), Platinum taq polymerase (0.6 U/20 μl reaction; Invitrogen), and SYBR Green (0.5× recommended concentration of the manufacturer; Molecular Probes, Eugene, OR), was aliquoted, the cDNA substrates were added, the mix was further aliquoted, and primers were added (C_f = 200 nM). Reactions were then split into triplicates for amplification in an MJ Research (Watertown, MA) Opticon DNA Engine with cycling parameters 95°C one time for 2 min, 95°C for 30 s/64°C for 45 s, and with fluorescence read at 78°C for 40 cycles. A melting curve and gel electrophoresis analysis verified that a single product was amplified in all reactions. For each run, the relative mRNA level was determined by the expression $2^{-\Delta\Delta Ct}$ (ΔCt (SK_{Ct}-$18S_{Ct}$) within each genotype, $\Delta\Delta Ct$ ($\Delta Ct_{\text{SK transgene}}$- $\Delta Ct_{\text{wild type}}$) (ABI Prism 7700 Sequence Detection System, user bulletin 2; Applied Biosystems, Foster City, CA). The mean and SEM of the value $2^{-\Delta\Delta Ct}$ were plotted for each SK mRNA across all runs.

Electrophysiological recordings

Hippocampal slices were prepared from 3- to 5-week-old SK2+/T or WT littermate mice. Mice were anesthetized with isoflurane and decapitated, and the brains were immediately removed and placed into ice-cold cutting solution (in mM: 110 sucrose, 60 NaCl, 2.5 KCl, 28 $NaHCO_3$, 1.25 NaH_2PO4, 0.5 $CaCl_2$, 7 $MgCl_2$, 5 glucose, and 0.6 ascorbate, equilibrated in 95% O_2 and 5% CO_2). Hippocampi were removed from the brain, placed onto a 4% agar block, and transferred to the slicing chamber. Transverse slices (400 μM) were cut with a Vibratome (Leica VT 1000S; Leica, Nussloch, Germany) and transferred to an incubation chamber containing artificial CSF (ACSF; in mM: 125 NaCl, 2.5 KCl, 21.4 $NaHCO_3$, 1.25 NaH_2PO4, 2 $CaCl_2$, 1 $MgCl_2$, and 11.1 glucose, equilibrated in 95% O_2 and 5% CO_2) maintained at 35°C for 30 min and then at room temperature for at least 90 min.

Whole-cell recordings. CA1 neurons were visualized using a microscope with infrared-differential interference contrast optics (Leica DMLFS) and a CCD camera (Sony, Tokyo, Japan). Recording pipettes were pulled from TW150F-4 thin-wall borosilicate glass (World Precision Instruments, Sarasota, FL). Pipettes had resistances of 1.5–3 MΩ and were filled with an intracellular solution containing the following (in mM): 140 $KMeSO_4$, 8 NaCl, 1 $MgCl_2$, 10 HEPES, 2 Mg-ATP, 0.4 Na_2-GTP, and 20 μM EGTA, pH 7.3, 290 mOsm). Whole-cell recordings were performed at room temperature (22–23°C), and during recordings, each slice was perfused continuously with ACSF equilibrated to 95% O_2/5% CO_2. Whole-cell patch-clamp currents were acquired with a Multiclamp 700A amplifier (Molecular Devices, Union City, CA), digitized using an ITC-16 converter (InstruTech, Greatneck, NY), and recorded onto a computer using Pulse software (HEKA Elektronik, Lambrecht, Germany).

For measurement of the IAHP, CA1 pyramidal neurons were voltage clamped at −55 mV, and tail currents were evoked with a depolarizing command to +20 mV for 100 ms, followed by a return to −55 mV for 10–20 s. After a stable baseline was established, apamin (100 nM; Calbiochem, La Jolla, CA) was applied to the bath, and the apamin-sensitive current was obtained by digital subtraction. Peak amplitudes of the apamin-sensitive current were measured at 100 ms after the return to −55 mV. Access resistance was compensated at 80%. Current recordings were filtered at 500 Hz and digitized at a sampling frequency of 1 kHz; the

records were filtered further off-line with a 300 Hz Gaussian filter (for one pass). To measure decay kinetics of the apamin-sensitive current, a single exponential was fit to subtracted (pre-apamin − post-apamin) currents. Data were analyzed with IGOR Pro software (Wavemetrics, Lake Oswego, OR) and are presented as mean ± SEM.

For measurement of EPSPs, synaptic potentials were recorded in whole-cell current-clamp mode at room temperature. A bipolar tungsten electrode (FHC, Bowdoinham, ME) was used to stimulate presynaptic axons in the stratum radiatum. Picrotoxin (0.1 mM) was added to reduce GABAergic contributions. The input resistance was determined from a ~7 pA hyperpolarizing current injection pulse given 800 ms after each synaptically evoked EPSP. Subthreshold EPSPs were elicited by 100 μs current injections that were approximately one-third of the stimulus required for evoking an action potential. No bias current was applied during EPSP recordings in current-clamp configuration. In some experiments, the magnitude of the apamin-induced increase in the EPSP elicited action potentials. Under these conditions, the stimulus strength was reduced to approximately one-quarter of threshold. Recordings were made using an Molecular Devices 200A amplifier interfaced to a Macintosh G4 with an ITC-16 computer interface (Instrutech). Data were filtered at 5 kHz and collected at a sample frequency of 20 kHz using Pulse software (HEKA Elektronik). All recordings used cells with a resting membrane potential less than −60 mV that did not change by >2 mV during an experiment and with a stable input resistance that did not change by >5%. Average resting membrane potentials were similar between genotypes (WT, −71.76 ± 0.36; SK2+/T, −68.75 ± 1.18; $p > 0.05$). The membrane potential was not corrected for liquid junction potential, which was 3.6 mV.

Field recordings. Schaffer collaterals were stimulated with a bipolar tungsten electrode (FHC) placed into area CA3. A recording pipette (2–4 MΩ) filled with ACSF was placed into the stratum radiatum of area CA1. Field EPSPs (fEPSPs) were recorded at 30 ± 1°C. After electrode placement, baseline synaptic transmission was monitored at 0.05 Hz, and a 10 min stable baseline was acquired before tetanization. LTP was induced with either three 50 Hz tetani (100 pulses at 0.1 Hz) or three 100 Hz tetani (100 pulses at 0.1 Hz). Both of these high-frequency stimulation protocols produced post-tetanic potentiation in all WT and SK2+/T slices recorded. LTD was induced with 1 Hz low-frequency stimulation applied for 20 min. In LTD experiments, 1 h after LTD induction, slices were tetanized with three 100 Hz tetani (100 pulses) at 0.1 Hz to ensure that bidirectional plasticity remained and that LTD was not attributable to cell death. Data were digitized (10 kHz sampling rate) with a National Instruments (Austin, TX) AD interface and analyzed using IGOR (Wavemetrics) on a Macintosh G3 computer (Apple Computers, Cupertino, CA). The maximal initial slope of the fEPSP was measured to monitor the strength of synaptic transmission, minimizing contamination by voltage-dependent events. Summary graphs were obtained by normalizing each experiment according to the average value of all points on the 10 min baseline. All points were aligned with respect to the start of the (LTP or LTD) induction protocol, and each experiment was divided into 1 min bins and averaged across experiments. The amount of potentiation or depression of the synaptic response was measured 30–40 min after conditioning.

Behavioral tasks

For all behavioral procedures, 8- to 10-week-old male mice were handled and weighed at least 2 d before the onset of the experiment.

Morris water maze. Naive male SK2+/T ($n = 14$) and WT littermate ($n = 17$) mice were used in the Morris water maze paradigm. The pool was constructed of white polyethylene (60 cm high, 109 cm diameter), and pool water (22–24°C) was clouded with the addition of nontoxic white Tempra paint. Mouse behavior was recorded with a video camera interfaced with the EthoVision 3.0 tracking system (Noldus, Leesburg, VA), permitting the acquisition of multiple behavioral parameters. Mice received 2 d of nonspatial training (one trial per day) to acclimate to the pool and submerged platform, 2 d of visible platform training (six trials per day) to examine sensorimotor function and striatal-dependent learning (McDonald and White, 1994), and 11 d of hidden platform training (four trials per day) to examine hippocampal-dependent spatial learning and memory (Morris et al., 1982). During nonspatial training, a clear Plexiglas platform (13 cm diameter) was located in the center of the pool and submerged 1 cm below the water surface, and a black curtain was drawn around the pool (0.5 m from pool) to block the animal's view of extra-maze visible cues in the room. Each nonspatial training trial was composed of placing the mouse onto the platform for 60 s and releasing it into the pool [adjacent to platform, north (N), south (S), east (E), and west (W)] four times to practice swimming and climbing onto the platform. During visible platform training, the curtain was opened to allow view of the large distal extra-maze visual cues (table, chair, posters affixed to the walls and to the open curtain, etc.), and a black Plexiglas platform (13 cm diameter) with a protruding flag was located just above the water's surface. The platform location and start site were randomized each trial. During hidden platform training, the platform was located in a fixed position in the center of the NE quadrant of the pool. The large distal visible cues were available to the mice during hidden platform training. Release points around the edge of the pool (N, S, E, and W) were randomized each day. Each mouse was allowed 60 s to reach the hidden platform, after which it was placed onto the platform. Mice remained on the platform for 30 s to view spatial cues and were placed into a holding cage for a 45 s intertrial interval. To examine spatial memory retention after training, mice received a probe test 24 h after the last training trial, during which the platform was removed from the pool and mice were allowed 60 s to search for the platform. A search ratio measure was calculated from probe test behavior for each mouse as the number of crossings into a 23.8 cm diameter circular zone around the platform location, divided by the total number of crossings into four equivalent zones (from each pool quadrant: N, S, E, and W). Both search ratio and percentage of time spent in the target quadrant were measured during the first 15 s of the final probe, which most accurately reflects search behavior.

Fear conditioning. Contextual and cued fear conditioning tasks were used to further assess the effects of SK2 overexpression on learning and memory. Learning in both contextual and cued fear conditioning tasks requires an intact amygdala, whereas contextual conditioning additionally requires hippocampal function (LeDoux, 1993). Contextual conditioning involves a learned association between an aversive unconditioned stimulus (e.g., footshock) and the environment in which it is presented (Kim and Fanselow, 1992; Phillips and LeDoux, 1992; Logue et al., 1997). This learned association is observed as an increase in freezing behavior in response to the training context (Kim and Fanselow, 1992). In contrast, cued fear conditioning involves the learned association between a discrete cue (e.g., tone) and the footshock, with subsequent freezing to the cue alone, and this learning does not require an intact hippocampus (LeDoux, 1993). In the present study, conditioned fear was examined in three replications, and data from these replications were combined because no effect of replication was found on any measure ($p > 0.05$). On the first day, naive SK2+/T (total $n = 42$) and WT littermate (total $n = 29$) mice received a context pre-exposure session, in which each mouse was allowed to explore one of four automated activity chambers (Freeze Monitor, 20 × 25 × 12.5 cm; San Diego Instruments, San Diego, CA) for 5 min. Each activity chamber was located inside a sound-attenuating box containing a small fan for white noise and a house light. Activity chambers contained removable steel shock grid floors and a clear Plexiglas ceiling and walls. The next day, each mouse was returned to the same chamber for conditioning, in which three 30 s tones (68 dB, 30 Hz) were presented with a coterminating 1 s footshock (0.5 mA). These tone–shock pairings began after a 60 s delay and were separated by a 180 s interstimulus interval. Chambers were cleaned with Liquinox detergent after each context pre-exposure and conditioning trial. To examine memory for contextual fear, each mouse was returned to the same chamber after a 24 h retention interval. No shock or tone was presented during this 5 min context test. To examine cued fear conditioning, a tone test was conducted ~2 h after the context test, in which each mouse was placed into a novel chamber that differed in location, odor (cleaned with 70% ethanol), sound (no fan), texture (smooth Plexiglas floor), and appearance (visual cues were added to chamber ceilings, floors, and walls; a Plexiglas divider diagonally bisected each chamber). During the tone test, the 30 s tone was presented twice after a 60 s delay and separated

by a 180 s interstimulus interval. Because mice express conditioned fear as a freezing response, the percentage of freezing was measured for each session.

Acoustic startle response and shock sensitivity were examined in separate cohorts of male SK2+/T and WT littermate mice to ensure that SK2 overexpression did not (1) impair ability to hear or respond to the tone stimulus or (2) affect unconditioned responses of the mice to the footshock stimulus. Acoustic startle response to a 60 ms, 10 kHz tone was recorded with the Coulbourn Instruments (Allentown, PA) acoustic startle response system. Strain gauge transducers coupled to the startle platform were used to detect the jumping response. Tones varied in intensity (0, 60, 80, and 100 dB) and were presented pseudo-randomly to male SK2+/T ($n = 6$) and WT littermate ($n = 7$) mice, 40 trials per day for 2 d, with varying intertrial intervals (15–55 s). The percentage of change in peak amplitude of responses to 60, 80, or 100 dB (relative to 0 dB) measured on days 1 and 2 were averaged for each mouse. To examine shock-sensitivity thresholds, male SK2+/T ($n = 6$) and WT littermate ($n = 6$) mice were placed into the conditioning chambers for 60 s and exposed to 0.5 s shocks every 120 s in order of increasing intensity (0.05, 0.25, 0.5, 0.63, and 0.75 mA). The magnitude of shock (in milliamperes) required to elicit a response (vocalization or running) was determined for each mouse.

Data analysis

All data are represented as mean ± SEM with significance set at $p > 0.05$. Real-time PCR was analyzed with a one-factor ANOVA. For electrophysiological recordings, field potential input–output relationships were analyzed with a three-factor ANOVA, with genotype, fiber volley amplitude, and genotype by fiber volley amplitude as predictors of fEPSP slope. Paired-pulse facilitation (PPF) ratio data were analyzed with repeated-measures ANOVA, and all other electrophysiological experiments were analyzed with two-tailed, independent-samples Student's *t* tests. For the Morris water maze, repeated-measures ANOVAs were used to assess behavior during visible and hidden platform training, analysis of covariance (ANCOVA) was used to examine differences during visible platform training, and two-tailed, independent-samples Student's *t* tests were used for all other comparisons. For fear conditioning and acoustic startle experiments, repeated-measures ANOVAs were used, with *post hoc* two-tailed Student's *t* tests where appropriate. Student's *t* tests were used to compare shock-sensitivity threshold measures.

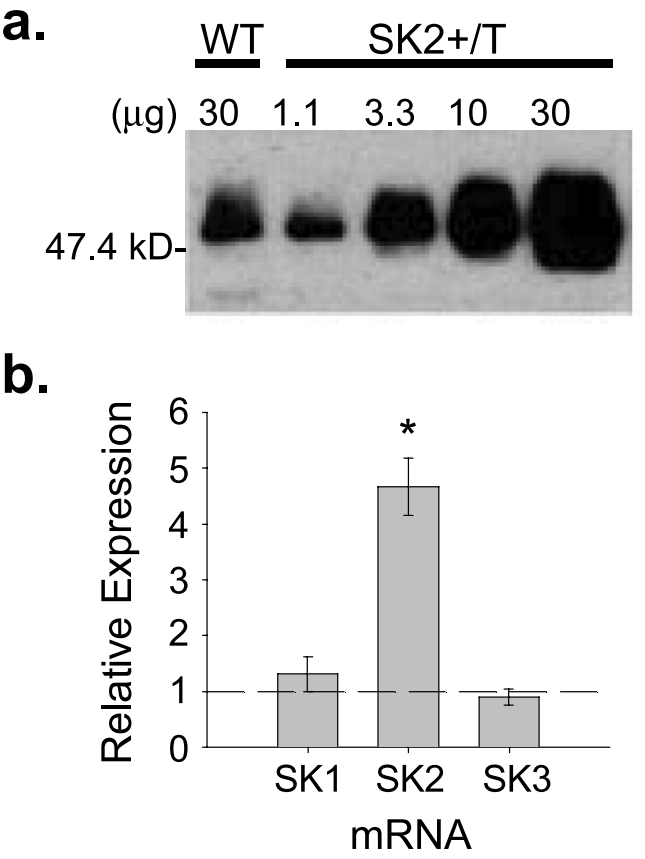

Figure 1. SK2+/T mice specifically overexpress SK2 channels. ***a***, Western blot reveals an ~10-fold overexpression of SK2 channels in SK2+/T mice. Membranes were prepared from whole-brain homogenate from WT or SK2+/T mice. Increasing amounts of brain membrane proteins from SK2+/T mice (1.1, 3.3, 10, and 30 μg) were loaded onto the gel for semiquantitative analysis. ***b***, Real-time PCR reveals that SK2 transcripts are overexpressed by ~4.5-fold, whereas SK1 and SK3 transcripts are expressed at WT levels in SK2+/T mice. Error bars indicate SEM. $^*p < 0.05$.

Results

SK2-overexpressing mice

Transgenic mice overexpressing SK2 channels were developed via insertion of a tetracycline-activated gene switch into the SK2 locus (Bond et al., 2000). Compared with WT littermate mice, in the absence of doxycycline, the SK2 protein and SK2 mRNA are overexpressed in heterozygotes (SK2+/T) ~10- and 4.5-fold as shown by Western blot and quantitative PCR, respectively (Fig. 1*a*,*b*) ($p < 0.001$). In addition, real-time PCR revealed that the SK1 and SK3 mRNA levels were unchanged in brains from SK2+/T mice, relative to WT mice (Fig. 1*b*).

We have shown previously that SK2 channels are necessary for apamin-sensitive currents in CA1 hippocampal neurons (Bond et al., 2004). Tail currents after 100 ms depolarizations to 20 mV were recorded from CA1 neurons in the whole-cell configuration. The addition of apamin to slices from SK2+/T mice revealed a fourfold increase in the amplitude of the apamin-sensitive component of the IAHP current recorded 100 ms after repolarization ($n = 7$; 359.55 ± 48.59 pA) relative to WT ($n = 13$; 87.03 ± 7.34 pA; $p < 0.001$) (Fig. 2*a–c*). SK2 overexpression did not alter the current recorded after 1 s (Fig. 2*c*, IsAHP), the decay kinetics of the apamin-sensitive current (WT, 325.38 ± 39.05 ms; SK2+/T, 356.86 ± 63.13 ms) (Fig. 2*d*), or the input resistance at −55 mV (WT, 276.82 ± 18.57 MΩ; SK2+/T, 305.46 ± 37.84 MΩ).

SK2 overexpression enhances SK channel-mediated restriction of glutamatergic activity in CA1

We reported previously that blocking SK channels with apamin in CA1 neurons increased the amplitude of synaptically evoked glutamatergic-mediated EPSPs in an NMDAR-dependent manner (Ngo-Anh et al., 2005). To determine whether the overexpression of SK2 channels would influence the magnitude of subthreshold synaptic events, 100 μs current pulses were applied to the stratum radiatum, and whole-cell EPSPs were recorded from CA1 neurons in hippocampal slices from WT (Fig. 3*a*, inset) and SK2+/T (Fig. 3*b*, inset) mice before and after apamin application (100 nM). Summary plots reveal that in slices from WT mice, apamin increased the peak EPSP amplitude by an average of 59 ± 5% of the control (Fig. 3*a*), whereas in slices from SK2+/T mice, apamin increased the peak EPSP amplitude by an average of 136 ± 8% of the control (Fig. 3*b*, Table 1) ($p < 0.02$).

These experiments were repeated using external solutions that contained lower concentrations of Mg^{2+} and higher concentrations of Ca^{2+}, conditions that augment NMDAR activation and further elevate Ca^{2+} influx through the NMDAR. Under these conditions, blocking SK channels with apamin increased the EPSP amplitude by an average of 217 ± 12% of the control in slices from SK2+/T mice (Table 1) compared with an increase in

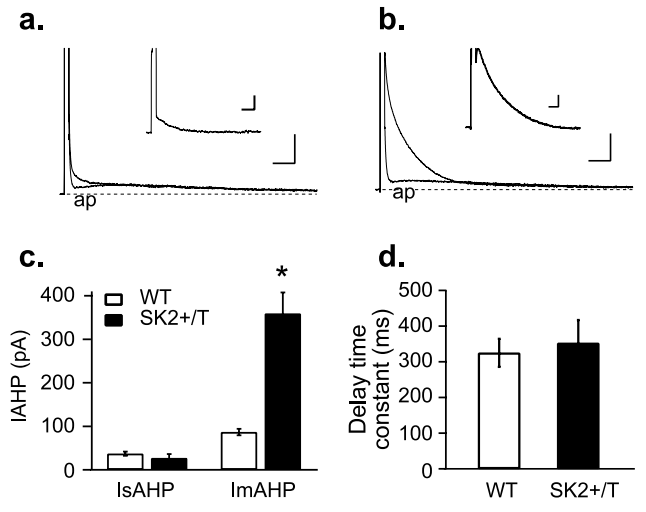

Figure 2. SK2 overexpression increases the amplitude of the apamin-sensitive current. ***a***, ***b***, Representative whole-cell recordings of CA1 neurons from WT (***a***) and SK2+/T (***b***) mice before and after apamin (ap) are shown. Cells were voltage clamped at 55 mV, and tail currents were elicited after a 100 ms depolarizing step to +20 mV. Calibration: 200 pA, 0.5 ms. The insets show the subtracted apamin-sensitive current (calibration: 100 pA, 200 ms). ***c***, Summary plot reveals that SK2 overexpression increases the amplitude of the apamin-sensitive current measured at 100 ms (ImAHP) by approximately fourfold but does not affect the apamin-insensitive current measured at 1 s (IsAHP). ***d***, SK2 overexpression does not alter the decay kinetics of the ImAHP. Error bars indicate SEM. $*p < 0.05$.

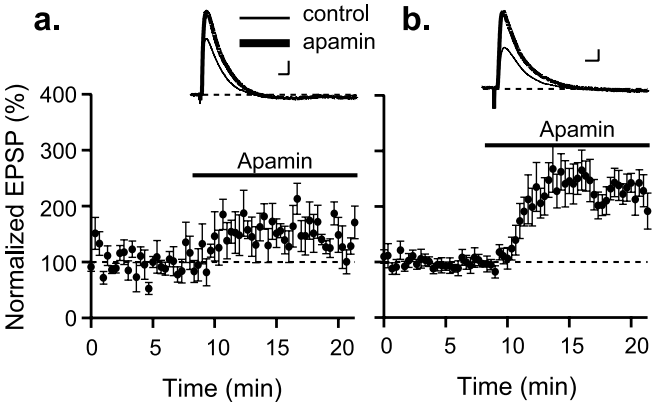

Figure 3. SK2 overexpression enhances the SK channel-mediated attenuation of the synaptically evoked glutamatergic EPSPs in CA1. An average EPSP waveform was derived from 20 EPSPs synaptically evoked in control condition in WT (***a***, inset) and SK2+/T (***b***, inset) mice before (thin line) and after (thick line) application of apamin. ***a***, Summary plot of the EPSP amplitude of WT mice under control condition relative to the baseline period during washin of apamin ($n = 5$ cells). ***b***, Summary plot of the EPSP amplitude of SK2+/T mice under control condition relative to the baseline period during washin of apamin ($n = 7$ cells). Calibration: 1 mV, 25 ms. The times of drug application are indicated by the horizontal bars. Error bars indicate SEM.

114 ± 11% of the control in WT slices ($p < 0.04$). Together, these data indicate that the overexpressed SK2 channels enhance the SK channel-mediated restriction of NMDAR activation that limits synaptically evoked excitatory events.

SK2 overexpression attenuates hippocampal synaptic plasticity

Previously, we have shown that blocking SK channels with apamin altered the modification threshold with which synaptic plasticity was induced in mouse hippocampal slices (Stackman et al., 2002). Therefore, we hypothesized that SK2 overexpression would affect the induction of synaptic plasticity. To test this, we stimulated CA3 Shaffer collateral synapses and recorded CA1 field potentials from hippocampal slices from SK2+/T mice and their WT littermates. Relative changes in synaptic strength were measured by the percentage of change in the maximum slope of fEPSPs. Induction of LTP with three 50 Hz tetani (100 pulses at 0.1 Hz) was significantly reduced in slices from SK2+/T mice ($n = 14$; 113.81 ± 3.67%), relative to WT slices 30–40 min after tetanization ($n = 7$; 133.06 ± 7.69%, $p = 0.018$) (Fig. 4*a*). These data indicate that SK2 overexpression attenuates the induction of hippocampal LTP. Induction of LTP with three 100 Hz trains (each 100 pulses at 0.1 Hz) was equivalent in WT ($n = 14$; 137.42 ± 5.43%) and SK2+/T ($n = 8$; 130.94 ± 13.12%) slices 30–40 min after tetanization (Fig. 4*b*) ($p > 0.05$). The magnitude of LTD induced by 1 Hz stimulation applied for 20 min was also equivalent in WT ($n = 7$; 80.73 ± 1.26%) and SK2+/T ($n = 8$; 76.58 ± 3.83%) slices 30–40 min after stimulation (Fig. 4*c*) ($p > 0.05$). Together, these data indicate that SK2 overexpression impairs the induction of LTP in a frequency-dependent manner without affecting the induction of LTD.

To determine whether these effects on synaptic plasticity could be explained by differences in CA1 basal synaptic transmission, we examined the input–output relationship of fiber volley amplitude to the fEPSP slope. fEPSPs were recorded from slices from WT ($n = 5$) and SK2+/T ($n = 7$) hippocampi over a range of stimulus intensities (2.5–10 μA) applied at 0.05 Hz. The maximum slope of the fEPSP was plotted versus the presynaptic fiber volley for each genotype (Fig. 5*a*). A three-factor ANOVA revealed that presynaptic fiber volley amplitude was a significant predictor of fEPSP slope (fiber volley, $p < 0.001$), and no differences in this relationship were found between genotypes (genotype by fiber volley, $p > 0.05$). To determine whether SK2 overexpression alters short-term plasticity mechanisms, we examined PPF in WT ($n = 5$) and SK2+/T ($n = 10$) slices. Paired pulses were delivered at 0.1 Hz, separated by intervals of 12, 20, 50, 100, and 200 ms. Repeated-measures ANOVA revealed no effect of genotype on the PPF ratio, calculated as the amplitude of the second fEPSP divided by the amplitude of the first fEPSP (Fig. 5*b*) (interval by genotype, $p > 0.05$). This suggests that the mechanisms of PPF, which are primarily presynaptic (Zucker, 1989), are not affected by SK2 overexpression. In addition, we examined possible effects of SK2 overexpression on the readily releasable pool of neurotransmitter vesicles by measuring the decline in fEPSPs over the 100 Hz tetanus. During this tetanus, the fEPSP will decline as the readily releasable pool of presynaptic vesicles is depleted. No differences were found between WT ($n = 15$) and SK2+/T ($n = 8$) slices in the decrease in the fEPSP slope of the 15th fEPSP relative to the first fEPSP (Fig. 5*c*) ($p > 0.05$), further supporting the view that SK2 overexpression does not alter presynaptic neurotransmitter release mechanisms. Together, these data indicate that the effect of SK2 overexpression on synaptic plasticity is not attributable to altered presynaptic mechanisms.

SK2 overexpression severely impairs spatial learning and memory in the Morris water maze

Previously, we reported that systemic apamin enhanced encoding of spatial memory in the Morris water maze task; apamin-treated mice required fewer training trials to learn the location of the hidden platform than control-treated mice (Stackman et al., 2002). Therefore, we hypothesized that SK2-overexpressing mice would require more training to learn the platform location in the water maze than WT mice. Before hidden platform training, mice were trained for 2 d (6 trials per day) to swim to a visible, cued platform, a hippocampal-independent learning task (McDonald

Table 1. Mean ± SEM properties of synaptically evoked EPSP responses in hippocampal slices from WT and SK2+/T mice

Genotype	Condition (*n*)	EPSP (mV)	Slope (mV/ms)	Half-width (ms)	Rise time (ms)
WT	Control	2.8 ± 0.2	0.67 ± 0.04	45 ± 1.4	3.9 ± 0.2
	Apamin (5)	4.6 ± 0.4 (159 ± 5%)	0.98 ± 0.1 (139 ± 7%)	45 ± 2.04	4.2 ± 0.1
SK2+/T	Control	3.3 ± 0.08	0.69 ± 0.04	51 ± 1.2	4.2 ± 0.1
	Apamin (7)	7.6 ± 0.2 (236 ± 8%)*	1.43 ± 0.05 (228 ± 13%)*	53 ± 1.8	4.9 ± 0.2
WT	Control (0.2 mM Mg^{2+})	4.2 ± 0.2	0.81 ± 0.04	43 ± 2.7	5.0 ± 0.2
	Apamin (6) (0.2 mM Mg^{2+})	8.5 ± 0.4 (214 ± 12%)	1.72 ± 0.08 (216 ± 5%)	42 ± 2.8	4.3 ± 0.2
SK2+/T	Control (0.2 mM Mg^{2+})	3.0 ± 0.1	0.63 ± 0.05	49 ± 2.0	4.7 ± 0.2
	Apamin (6) (0.2 mM Mg^{2+})	9.2 ± 0.5 (318 ± 12%)*	1.77 ± 0.13 (327 ± 16%)*	46 ± 1.9	4.5 ± 0.4

Slope was defined as the maximum rate of rise of the EPSP. Half-width refers to the width of the EPSP measured at 50% of the maximum amplitude. Rise time refers to the time required for the EPSP to rise from 20 to 80% of the maximum amplitude. The percentage of control values for each condition is presented in parentheses. *$p < 0.05$ compared with the respective value from WT slices.

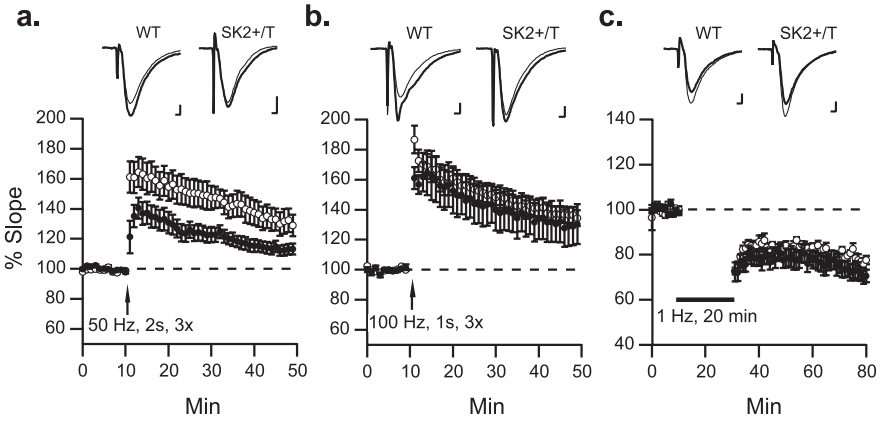

Figure 4. SK2 overexpression impairs the induction of synaptic plasticity in a frequency-dependent manner. Field potentials were recorded from the CA1 region of WT (○) and SK2+/T (●) hippocampal slices. Representative traces from baseline (thin line) and at 50 min after tetanus (thick line) are displayed at the top of the figure from each experiment (calibration: 0.25 mV, 2 ms). ***a***, LTP was induced with three tetani consisting of 100 pulses delivered at 50 Hz (0.1 Hz). Slices from SK2+/T mice exhibited significantly less LTP 30–40 min after 50 Hz stimulation than slices from WT mice ($p = 0.018$). ***b***, SK2 overexpression did not disrupt 100 Hz LTP induced with three tetani consisting of 100 pulses delivered at 100 Hz (0.1 Hz). ***c***, SK2 overexpression did not disrupt LTD induced with low-frequency stimulation of 1 Hz for 20 min. Error bars indicate SEM.

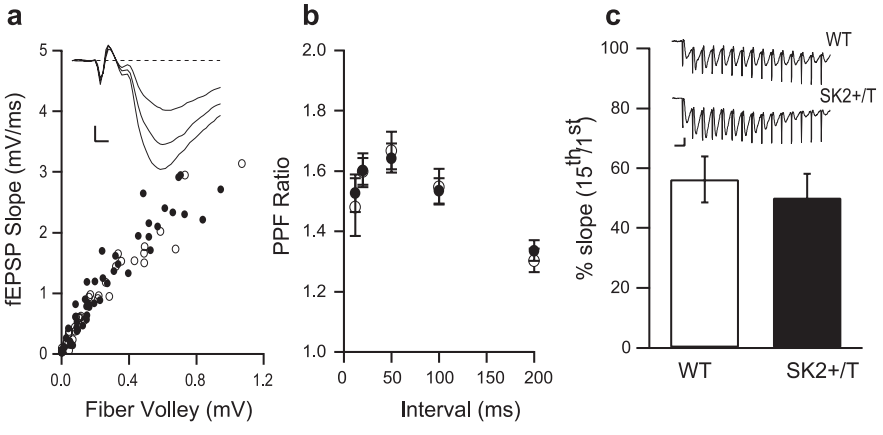

Figure 5. SK2 overexpression does not alter basal synaptic transmission or presynaptic release mechanisms. ***a***, fEPSP slope measures were plotted against the corresponding fiber volley amplitude evoked by stimulation of the Schaffer collaterals with increasing intensity. The inset depicts representative traces from an SK2+/T slice (calibration: 0.25 mV, 2 ms). For each genotype, fiber volley amplitude was a significant predictor for fEPSP slope ($p < 0.001$), and there was no genotype effect on synaptic transmission properties. ***b***, SK2 overexpression did not alter the PPF ratio ($p > 0.05$). ***c***, Decline in fEPSPs during 100 Hz stimulation was not altered by SK2 overexpression ($p > 0.05$). The inset depicts representative traces (calibration: 0.25 mV, 5 ms). Error bars indicate SEM. ○, WT; ●, SK2+/T.

and White, 1994). The cumulative distance of the mouse to the target platform (CDT) reflects platform search efficiency (Gallagher et al., 1993) and was recorded each trial. Although analysis of the CDT did not reveal a significant genotypic difference in learning the visible platform task (genotype-by-trial block: $F_{(2,29)} = 2.01$; $p > 0.05$) (Fig. 6*a*), a significant main effect of genotype was found for the CDT ($F_{(1,29)} = 8.00$; $p = 0.008$). SK+/T mice also swam slower than WT mice in the visible platform task (Fig. 6*b*) (genotype: $F_{(1,29)} = 13.64$; $p = 0.001$), and when the visible platform CDT data were reanalyzed with swim speed as a covariate, the main effect of genotype was not significant (ANCOVA: $F_{(2,25)} = 1.73$; $p > 0.05$). This result indicates that genotypic differences in the CDT during visible platform training were attributable to differences in swim speed. Together, the visible platform data indicate that SK2 overexpression does not obviously impair vision, swimming ability, or striatal-dependent learning (McDonald and White, 1994).

In the hippocampal-dependent version of the Morris water maze task, mice use spatial cues to learn the fixed location of a hidden platform. Over successive training trials, mice encode a hippocampal-dependent spatial map that permits efficient and biased search behavior during subsequent probe tests. SK2+/T and WT mice were trained in the hidden platform task beginning 24 h after completion of visible platform training. On each trial (four per day), mice were placed into the pool and allowed 60 s to escape onto the hidden platform. During hidden platform training, SK2+/T mice exhibited significantly longer CDT measures (Fig. 6*c*) ($F_{(1,29)} = 18.06$; $p < 0.001$) and longer escape latencies (data not shown; $F_{(1,29)} = 19.25$; $p < 0.001$) compared with WT mice. Importantly, there were no genotypic differences in swimming speed in the hidden platform task (Fig. 6*d*) ($F_{(1,29)} = 0.56$; $p > 0.05$). In addition, although WT mice attained asymptotic CDT scores by their fifth day of hidden platform training, the SK2+/T mice never reached a similar performance level even after 11 d of training (Fig. 6*c*). Although the performance of SK2+/T and WT mice improved at a similar rate over training (genotype-by-trial block: $F_{(10,290)} = 1.65$; $p > 0.05$), CDT scores differed considerably between genotypes at the conclusion of training. Together, these results demonstrate deficient

spatial learning by SK2+/T mice and suggest that the SK2+/T mice were using a means of locating the hidden platform that was distinct from the spatial mapping strategy of their WT littermates.

SK2+/T mice exhibited longer CDT measures than WT mice ($t_{(29)} = 3.62$; $p = 0.001$) during the first day of hidden platform training. This initial difference in hidden platform task performance likely reflects an impairment of the SK2+/T mice in the efficiency of switching from the task requirements of the visible platform to those of the hidden platform task. In support of this view, a separate cohort of naive SK2+/T ($n = 12$) and WT littermate ($n = 6$) mice exhibited equivalent CDT scores on the first day of hidden platform training, when this training was not preceded by visible platform training (supplemental Fig. S1*a*, available at www.jneurosci.org as supplemental material) (WT, 11,534.98 ± 2789.26 cm; SK2+/T, 12,209.17 ± 1362.05 cm; $t_{(16)} = -0.247$; $p > 0.05$). As in the present study, this second cohort of SK2+/T mice exhibited impaired spatial learning and impaired spatial memory during the probe test (supplemental Fig. S1*a*,*b*, respectively, available at www.jneurosci.org as supplemental material) in the Morris water maze task.

The learning and memory impairments of SK2+/T mice were further revealed during the final probe test, administered 24 h after the last training trial (Fig. 6*e–h*). WT mice exhibited a strong spatial bias in their search behavior during the final probe test, with 51.21 ± 4.43% of time spent in the quadrant of the pool where the platform was located during training (Fig. 6*e*), and a search ratio significantly above chance performance (Fig. 6*f*) ($t_{(16)} = 5.80$; $p > 0.001$). Consistent with the quantitative analyses, representative traces of swim paths from the probe test indicate that WT mice used an allocentric spatial mapping strategy, conducting a spatially biased search in the region of the pool that previously contained the platform (Fig. 6*g*). However, even after this extensive training protocol, SK2+/T mice spent significantly less time in the quadrant of the pool where the platform was located during training (Fig. 6*e*) (24.48 ± 6.14%) than did WT mice ($t_{(29)} = -4.01$; $p < 0.001$). In addition, the search ratio measures (Fig. 6*f*) indicate that SK2+/T mice searched less accurately than WT mice ($t_{(29)} = -4.13$; $p < 0.001$) and failed to exhibit a significant spatial bias for the platform location ($t_{(13)} = 0.29$; $p > 0.05$). Representative swim paths of SK2+/T mice (Fig. 6*h*) further demonstrate the lack of an obvious spatial bias to their search behavior and indicate that some mice exhibited an alternative egocentric search strategy (such as circular swimming a fixed distance from the wall of the pool) (Fig. 6*h*, right trace). Such egocentric search strategies are often used by water-maze-trained rodents with impaired hippocampal function (Morris et al., 1982; Riedel et al., 1999). These data suggest that SK2+/T mice failed to use a hippocampal-dependent spatial mapping strategy to find the hidden platform in the water maze. Together, these data demonstrate that SK2 overexpression severely impairs spatial learning and memory in the hippocampal-dependent version of the Morris water maze.

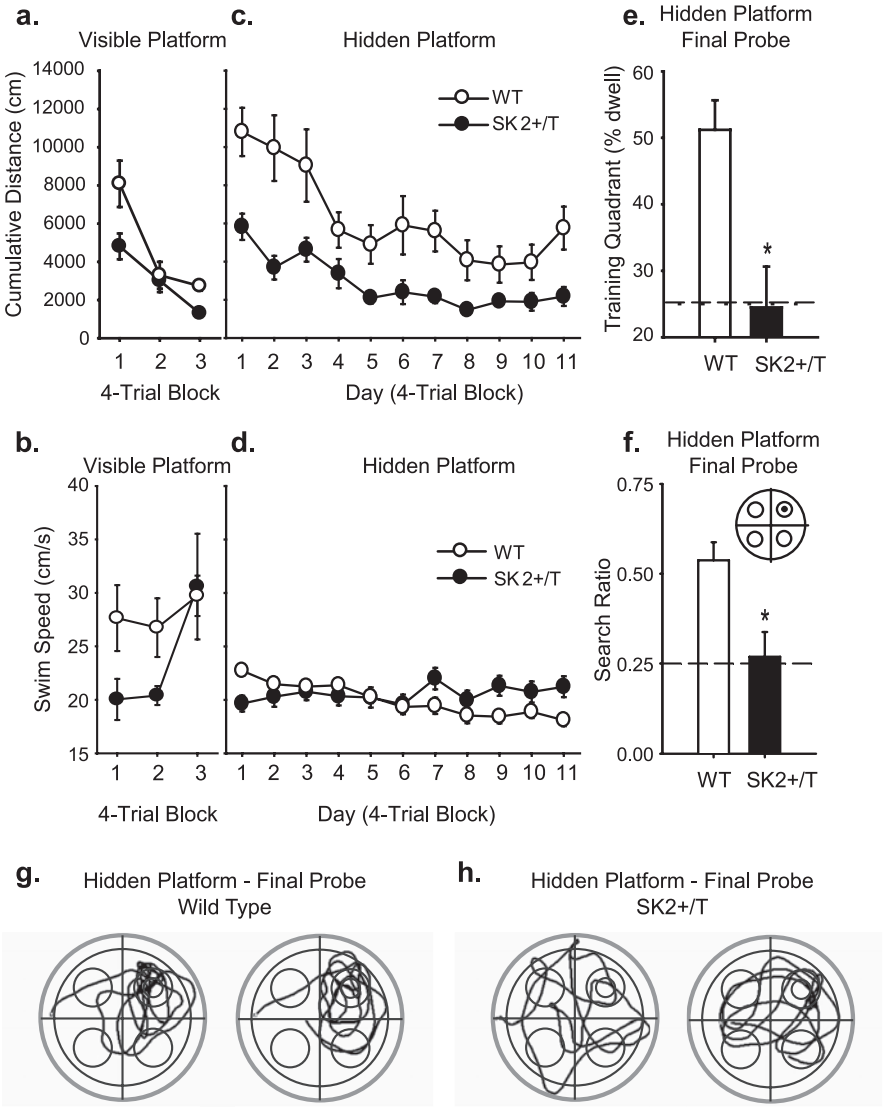

Figure 6. SK2 overexpression impairs hippocampal-dependent learning and memory in the Morris water maze. ***a***, ***b***, Learning in the hippocampal-independent visible platform water maze task was not different between WT (○) and SK2+/T (●) mice as assessed by CDT with swim speed as a covariate (***a***), ANCOVA ($p > 0.05$), although SK2+/T mice swam slower than WT mice (***b***). ***c***, ***d***, Learning in the hippocampal-dependent hidden platform water maze is significantly impaired in SK2+/T mice relative to WT mice (c, $p < 0.001$), and there were no genotypic differences in swim speed in this version of the task (***d***, $p > 0.05$). ***e***, During the final probe test 24 h after the last hidden platform training trial, SK2+/T mice spent significantly less time in the quadrant of pool relative to the WT mice ($p < 0.001$). ***f***, Search ratios computed from final probe test data indicate that SK2+/T mice failed to show a spatial bias for the platform location; search ratios were equivalent to chance performance ($p > 0.05$) and were significantly lower than WT ratios ($p < 0.001$), indicating that SK2 overexpression severely restricts learning and remembering the location of the hidden platform. Search ratios were defined as the frequency of crossings through a circular zone around the platform location (***f***, inset) divided by the frequency of crossings into all four circular zones. ***g***, ***h***, Representative tracings of swim paths of two WT mice (***g***) and two SK2+/T mice (***h***) during the final probe test. Fourteen of the 17 WT mice exhibited platform search patterns similar to that depicted in ***g***, which were characterized as accurate search. In contrast, 8 of the 14 SK2+/T mice exhibited search patterns similar to those depicted in ***h***, which were characterized as random search (left trace) or egocentric search (right trace). Error bars indicate SEM.

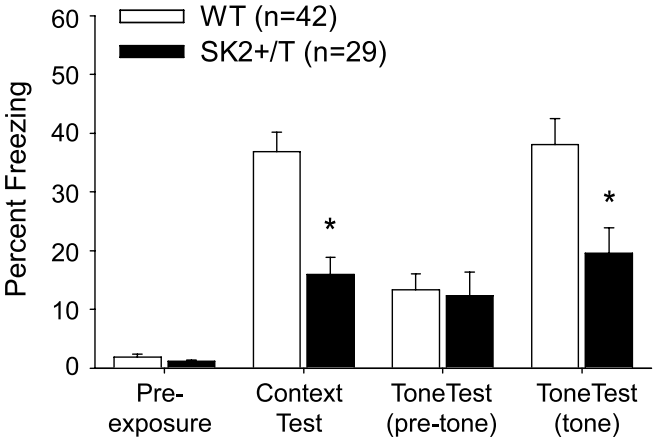

Figure 7. SK2 overexpression impairs contextual and cued fear conditioning. There was no genotypic difference in freezing behavior between WT and SK2+/T mice during the 5 min context pre-exposure session. During the context test 24 h after conditioning, both genotypes exhibited conditioned fear demonstrated by increased frequency relative to the pre-exposure session ($p < 0.001$), although percentage of freezing was significantly reduced in SK2+/T mice compared with WT controls ($p < 0.001$), indicating impaired contextual conditioning in SK2+/T mice. During the tone test, before the tone was presented (minute 1), there were no differences in percentage of freezing between genotypes ($p > 0.05$), indicating SK2 overexpression did not alter baseline freezing behavior. However, during the tone test, SK2+/T mice exhibited less freezing in response to the tone compared with WT mice (minute 2; $p = 0.004$), indicating that SK2 overexpression also impaired cued fear conditioning. Error bars indicate SEM. *$p < 0.05$.

SK2 overexpression impairs contextual and cued fear conditioning

The contextual fear-conditioning paradigm was used to further examine the effects of SK2 overexpression on hippocampal learning and memory. In contextual fear conditioning, the mouse forms an association between an aversive event and the distinctive context in which that event took place. Mice will exhibit conditioned fear responses when they are returned to the context, such as freezing (the absence of all movement, except for respiration). This form of learning is dependent on the hippocampus (Kim and Fanselow, 1992; Phillips and LeDoux, 1992). WT ($n = 42$) and SK2+/T ($n = 29$) mice were first exposed to the conditioning chamber for a 5 min context pre-exposure session. During conditioning 24 h later, mice were returned to the same chamber and received three pairings of a 30 s auditory tone and a 1 s 0.5 mA footshock. Twenty-four hours after conditioning, mice were returned to the same chamber for a 5 min context test. Both genotypes exhibited conditioned fear to the context during the context test, expressed as an increase in percentage of freezing relative to the pre-exposure session (Fig. 7) (session: $F_{(1,69)} = 119.14$; $p < 0.001$). In addition, a significant genotype-by-session interaction was found ($F_{(1,69)} = 19.69$; $p < 0.001$), and *post hoc* comparisons revealed that SK2+/T mice exhibited significantly less percentage of freezing to the context than WT mice ($t_{(69)} = 4.49$; $p < 0.001$) during the context test, indicating impaired contextual fear conditioning.

SK2 channels are also expressed throughout the amygdala and may modulate amygdala-dependent learning and memory. Lesions of the amygdala disrupt fear conditioning to auditory stimuli (Phillips and LeDoux, 1992). Therefore, we also examined retention of amygdala-dependent cued fear conditioning in SK2+/T and WT littermate mice. One hour after the context test, mice were placed into a novel environment for the tone test, in which they were presented with the tone after a 1 min delay. Both genotypes exhibited conditioned fear to the tone, expressed as increased percentage of freezing in min 2 (after the tone presentation) relative to min 1 (before the tone presentation) (Fig. 7) (minute: $F_{(1,69)} = 28.66$; $p < 0.001$). A significant genotype-by-minute interaction was also found ($F_{(1,69)} = 8.69$; $p = 0.004$), and *post hoc* comparisons revealed that SK2+/T mice exhibited less freezing in response to the tone (min 2) than WT mice (Fig. 7) ($t_{(69)} = 2.90$; $p = 0.005$), suggesting that SK2 overexpression impaired cued fear conditioning. Importantly, no differences in percentage of freezing were found between genotypes during the first minute of the tone test (before tone presentation), indicating that SK2 overexpression did not affect baseline freezing behavior (Fig. 7) ($t_{(69)} = 0.20$; $p > 0.05$).

To ensure that SK2+/T mice were equally sensitive to the acoustic and footshock stimuli used in this delay fear-conditioning procedure, separate cohorts of mice (WT, $n = 6–7$; SK2+/T, $n = 6$) were tested for acoustic startle response and shock sensitivity. Repeated-measures ANOVA revealed no effect of genotype on the percentage of change in the peak response with a 60 dB (WT, 123.85 ± 2.13%; SK2+/T, 120.66 ± 2.38%), 80 dB (WT, 142.12 ± 3.34%; SK2+/T, 144.16 ± 3.17%), or 100 dB (WT, 142.88 ± 2.76%; SK2+/T, 146.99 ± 3.57%) tone, indicating that tone salience was equivalent for SK2+/T and WT mice ($F_{(1,198)} = 0.09$; $p > 0.05$). The shock threshold (in milliamperes) required to elicit a response, determined for each mouse during shock-sensitivity testing, were not different between genotypes (WT, 0.32 ± 0.03 mA; SK2+/T, 0.32 ± 0.04 mA; $t_{(10)} = 0.37$; $p > 0.05$). Together, these data show that SK2-overexpressing mice have deficits in memory for hippocampal- and amygdala-dependent conditioned fear responses. Importantly, these deficits are not likely attributable to sensory or motor differences between the genotypes.

Discussion

Blocking SK channels with apamin enhances hippocampal synaptic plasticity (Behnisch and Reymann, 1998; Stackman et al., 2002; Kramár et al., 2004) and memory encoding (Stackman et al., 2002). The present study demonstrates that SK2 channels selectively regulate the hippocampal physiology and synaptic plasticity that may underlie spatial and contextual memory formation. SK2 overexpression increased the apamin-sensitive current in hippocampal CA1 neurons, decreased synaptically evoked glutamatergic EPSPs, attenuated 50 Hz LTP in hippocampal slices, and drastically impaired learning and memory in two hippocampal-dependent tasks. SK2 overexpression did not alter basal synaptic transmission or presynaptic release mechanisms (Fig. 5). These effects are not likely attributable to differences in the SK2 expression pattern, because the endogenous promoter drives expression in SK2+/T mice, nor are these effects as a result of compensatory changes in SK1 or SK3 channel expression (Fig. 1*b*).

In agreement with the observed frequency-dependent impairment of LTP induction, we found that SK2 overexpression disrupted hippocampal-dependent learning and memory in both the Morris water maze (Fig. 6) and a contextual fear-conditioning paradigm (Fig. 7). In the Morris water maze, SK2+/T mice exhibited profound learning impairments and were unable to learn and remember the platform location even after 11 d of training. Cumulative distance to platform measures of the SK2+/T mice did improve over the course of hidden platform training, yet not to the degree of the WT mice. Examination of behavior of SK2+/T mice during the final probe test revealed a marked lack of the characteristic biased search in the location of the pool that previously contained the platform. These data are

consistent with the view that SK2 channel overexpression prevented the hippocampal-based encoding and retention of a spatial representation of the position of the platform with respect to extra-maze cues. It is unlikely that the observed effects were attributable to impaired sensorimotor function, because SK2+/T mice were able to learn to locate a visible platform in the striatal-dependent water maze task.

SK2 overexpression disrupted both hippocampal-dependent contextual fear conditioning and hippocampal-independent cued fear conditioning. These impairments are not likely attributable to sensorimotor differences, because SK2+/T mice exhibited baseline freezing behavior, acoustic startle responses, and shock sensitivities equivalent to those of WT mice. The impairment of SK2+/T mice in cued fear conditioning, an amygdala-dependent task (Davis, 1994), is consistent with the fact that SK2 channels are expressed throughout the amygdala (Sailer et al., 2002, 2004). Furthermore, cued fear conditioning has been associated with LTP of the lateral amygdala (Rogan and LeDoux, 1995; Rogan et al., 1997), and SK channels in the lateral amygdala regulate the activity of NMDARs (Faber et al., 2005). These data suggest a similar mechanism for SK channel-mediated regulation of hippocampal-dependent and amygdala-dependent synaptic plasticity and learning. A number of previous studies have revealed that treatment of rats and mice with the SK channel antagonist apamin can facilitate the acquisition of several learning tasks (for review, see Tzounopoulos and Stackman, 2003). We found previously that apamin facilitated the encoding of hippocampal memory in both spatial and object memory tasks (Stackman et al., 2002). The present findings suggest that overexpression of SK2 channels may delay acquisition of hippocampal-dependent memory and that SK2 channels likely contribute to the cognitive effects of apamin.

There are at least two mechanisms by which the overexpression of SK2 channels might affect hippocampal function. Whole-cell recordings revealed that the apamin-sensitive current in CA1 neurons, which contributes to the afterhyperpolarization, was significantly greater in SK2-overexpressing mice than in WT mice. The increase in the apamin-sensitive current in CA1 may affect neuronal excitability at the soma and subsequently affect learning and memory (Disterhoft et al., 1988; McEchron et al., 2001; Oh et al., 2003). A second and more direct mechanism by which SK2 channels may affect the induction of synaptic plasticity is via a Ca^{2+}-mediated feedback loop between NMDARs and SK channels in the dendritic spines of CA1 neurons. The Ca^{2+} influx through NMDARs contributes at least 75% of the postsynaptic Ca^{2+} transient that underlies changes in synaptic strength (Nevian and Sakmann, 2004). The synaptically evoked Ca^{2+} influx activates SK channels located within 25–50 nm of NMDARs in the spine (Ngo-Anh et al., 2005). The resulting SK channel activation partially shunts the AMPA receptor-mediated depolarization, favoring the voltage-dependent Mg^{2+} block of NMDARs and thereby attenuating Ca^{2+} influx. In this model, SK2 overexpression might be expected to increase the SK component of the EPSP, and indeed we found that the SK channel-mediated restriction of glutamatergic EPSPs was significantly enhanced compared with WT controls (Fig. 3). Therefore, these data are consistent with our model, in which SK channels are distributed to the dendritic spine compartments where they couple to NMDAR Ca^{2+} influx. Moreover, these results are consistent with the proposed mechanism whereby SK channels regulate the induction of synaptic plasticity through the modulation of NMDAR activation and suggest that these cellular mechanisms underlie the observed alterations in hippocampal-dependent memory.

These results extend previous findings that SK channels regulate hippocampal synaptic plasticity, learning, and memory and provide evidence that SK2 channels mediate these processes. However, we cannot conclude from these data that homomeric SK2 channels are the only SK channels that contribute to the regulation of hippocampal function. SK3 and SK1 channels are also expressed in the rodent hippocampus, albeit at lower levels than SK2 channels (Stocker and Pedarzani, 2000; Tacconi et al., 2001; Sailer et al., 2002). There is evidence that SK3 channel expression levels influence memory (Blank et al., 2003). However, transgenic mice with conditional overexpression or knockdown of SK3 (Bond et al., 2004) do not exhibit altered hippocampal-dependent spatial memory in the Morris water maze (our unpublished results). In addition, SK3 channels have been shown to be localized to presynaptic terminals in cultured mouse hippocampal neurons (Obermair et al., 2003), suggesting that any SK3 contribution to hippocampal function would occur through presynaptic mechanisms. Furthermore, the apamin-sensitive current in CA1 neurons is abolished in SK2-null mice, yet not significantly affected in mice lacking SK1 or SK3 channels (Bond et al., 2004). Consistent with this, results from the present study suggest that SK2 channels may play an important role in the modulation of hippocampal synaptic plasticity, learning and memory.

References

Behnisch T, Reymann KG (1998) Inhibition of apamin-sensitive calcium dependent potassium channels facilitate the induction of long-term potentiation in the CA1 region of rat hippocampus in vitro. Neurosci Lett 253:91–94.

Blank T, Nijholt I, Kye MJ, Radulovic J, Spiess J (2003) Small-conductance, Ca^{2+}-activated K^+ channel SK3 generates age-related memory and LTP deficits. Nat Neurosci 6:911–912.

Bond CT, Sprengel R, Bissonnette JM, Kaufmann WA, Pribnow D, Neelands T, Storck T, Baetscher M, Jerecic J, Maylie J, Knaus HG, Seeburg PH, Adelman JP (2000) Respiration and parturition affected by conditional overexpression of the Ca^{2+}-activated K^+ channel subunit, SK3. Science 289:1942–1946.

Bond CT, Herson PS, Strassmaier T, Hammond RS, Stackman RW, Maylie J, Adelman JP (2004) Small conductance Ca^{2+}-activated K^+ channel knock-out mice reveal the identity of calcium-dependent afterhyperpolarization currents. J Neurosci 24:5301–5306.

Cai X, Liang CW, Muralidharan S, Kao JP, Tang CM, Thompson SM (2004) Unique roles of SK and Kv4.2 potassium channels in dendritic integration. Neuron 44:351–364.

Davis M (1994) The role of the amygdala in emotional learning. Int Rev Neurobiol 36:225–266.

Disterhoft JF, Golden DT, Read HL, Coulter DA, Alkon DL (1988) AHP reductions in rabbit hippocampal neurons during conditioning correlate with acquisition of the learned response. Brain Res 462:118–125.

Eichenbaum H (1999) The hippocampus and mechanisms of declarative memory. Behav Brain Res 103:123–133.

Eichenbaum H (2000) A cortical-hippocampal system for declarative memory. Nat Rev Neurosci 1:41–50.

Faber ES, Delaney AJ, Sah P (2005) SK channels regulate excitatory synaptic transmission and plasticity in the lateral amygdala. Nat Neurosci 8:635–641.

Gallagher M, Burwell R, Burchinal M (1993) Severity of spatial learning impairment in aging: development of a learning index for performance in the Morris water maze. Behav Neurosci 107:618–626.

Kim JJ, Fanselow MS (1992) Modality-specific retrograde amnesia of fear. Science 256:675–677.

Kohler M, Hirschberg B, Bond CT, Kinzie JM, Marrion NV, Maylie J, Adelman JP (1996) Small-conductance, calcium-activated potassium channels from mammalian brain. Science 273:1709–1714.

Kramár EA, Lin B, Lin CY, Arai AC, Gall CM, Lynch G (2004) A novel

mechanism for the facilitation of theta-induced long-term potentiation by brain-derived neurotrophic factor. J Neurosci 24:5151–5161.

LeDoux JE (1993) Emotional memory systems in the brain. Behav Brain Res 58:69–79.

Logue SF, Paylor R, Wehner JM (1997) Hippocampal lesions cause learning deficits in inbred mice in the Morris water maze and conditioned-fear task. Behav Neurosci 111:104–113.

Malenka RC, Nicoll RA (1999) Long-term potentiation–a decade of progress? Science 285:1870–1874.

McDonald RJ, White NM (1994) Parallel information processing in the water maze: evidence for independent memory systems involving dorsal striatum and hippocampus. Behav Neural Biol 61:260–270.

McEchron MD, Weible AP, Disterhoft JF (2001) Aging and learning-specific changes in single-neuron activity in CA1 hippocampus during rabbit trace eyeblink conditioning. J Neurophysiol 86:1839–1857.

Morris RGM, Garrud P, Rawlins JNP, O'Keefe J (1982) Place navigation impaired in rats with hippocampal lesions. Nature 297:681–683.

Nevian T, Sakmann B (2004) Single spine Ca^{2+} signals evoked by coincident EPSPs and backpropagating action potentials in spiny stellate cells of layer 4 in the juvenile rat somatosensory barrel cortex. J Neurosci 24:1689–1699.

Ngo-Anh TJ, Bloodgood BL, Lin M, Sabatini BL, Maylie J, Adelman JP (2005) SK channels and NMDA receptors form a Ca^{2+}-mediated feedback loop in dendritic spines. Nat Neurosci 8:642–649.

Obermair GJ, Kaufmann WA, Knaus HG, Flucher BE (2003) The small conductance Ca^{2+}-activated K^+ channel SK3 is localized in nerve terminals of excitatory synapses of cultured mouse hippocampal neurons. Eur J Neurosci 17:721–731.

Oh MM, Kuo AG, Wu WW, Sametsky EA, Disterhoft JF (2003) Watermaze learning enhances excitability of CA1 pyramidal neurons. J Neurophysiol 90:2171–2179.

Phillips RG, LeDoux JE (1992) Differential contribution of amygdala and hippocampus to cued and contextual fear conditioning. Behav Neurosci 106:274–285.

Riedel G, Micheau J, Lam AG, Roloff E, Martin SJ, Bridge H, Hoz L, Poeschel B, McCulloch J, Morris RG (1999) Reversible neural inactivation reveals hippocampal participation in several memory processes. Nat Neurosci 2:898–905.

Rogan MT, LeDoux JE (1995) LTP is accompanied by commensurate enhancement of auditory-evoked responses in a fear conditioning circuit. Neuron 15:127–136.

Rogan MT, Staubli UV, LeDoux JE (1997) Fear conditioning induces associative long-term potentiation in the amygdala. Nature 390:604–607.

Sailer CA, Hu H, Kaufmann WA, Trieb M, Schwarzer C, Storm JF, Knaus HG (2002) Regional differences in distribution and functional expression of small-conductance Ca^{2+}-activated K^+ channels in rat brain. J Neurosci 22:9698–9707.

Sailer CA, Kaufmann WA, Marksteiner J, Knaus HG (2004) Comparative immunohistochemical distribution of three small-conductance Ca^{2+}-activated potassium channel subunits, SK1, SK2, and SK3 in mouse brain. Mol Cell Neurosci 26:458–469.

Squire LR (1992) Memory and the hippocampus: a synthesis from findings with rats, monkeys, and humans. Psychol Rev 99:195–231.

Stackman RW, Hammond RS, Linardatos E, Gerlach A, Maylie J, Adelman JP, Tzounopoulos T (2002) Small conductance Ca^{2+}-activated K^+ channels modulate synaptic plasticity and memory encoding. J Neurosci 22:10163–10171.

Stocker M, Pedarzani P (2000) Differential distribution of three Ca^{2+}-activated K^+ channel subunits, SK1, SK2, and SK3, in the adult rat central nervous system. Mol Cell Neurosci 15:476–493.

Stocker M, Krause M, Pedarzani P (1999) An apamin-sensitive Ca^{2+}-activated K^+ current in hippocampal pyramidal neurons. Proc Natl Acad Sci USA 96:4662–4667.

Strassmaier T, Bond CT, Sailer CA, Knaus HG, Maylie J, Adelman JP (2005) A novel isoform of SK2 assembles with other SK subunits in mouse brain. J Biol Chem 280:21231–21236.

Tacconi S, Carletti R, Bunnemann B, Plumpton C, Merlo Pich E, Terstappen GC (2001) Distribution of the messenger RNA for the small conductance calcium-activated potassium channel SK3 in the adult rat brain and correlation with immunoreactivity. Neuroscience 102:209–215.

Tzounopoulos T, Stackman RW (2003) Enhancing synaptic plasticity and memory: a role for small conductance Ca^{2+}-activated K^+ channels. Neuroscientist 9:434–439.

Zucker RS (1989) Short-term synaptic plasticity. Annu Rev Neurosci 12:13–31.